D6.4 Novel methodologies for damage detection and assessment along the CH assets and the surrounding disaster affected area

Deliverable number	**D6.4**
Deliverable title	**Novel methodologies for damage detection and assessment along the CH assets and the surrounding disaster affected area**
Nature[1]	**Other**
Dissemination Level [2]	**PU**
Authors (email) Institution	Karathanassi V. karathan@survey.ntua.gr, Georgopoulos A. drag@central.ntua.gr, Kolokoussis P. pol@survey.ntua.gr Skamantzari M. sk.margarita@hotmail.com Karamvassis Kl. Karamvasis_K@hotmail.com **NTUA**
Editor (email) Institution	Karathanassi V. karathan@survey.ntua.gr **NTUA**
Leading partner	**NTUA**
Participating partners	
Official submission date:	**31/05/2021**
Actual submission date:	

[1] **R**=Document, report; **DEM**=Demonstrator, pilot, prototype; **DEC**=website, patent fillings, videos, etc.; **OTHER**=other

[2] **PU**=Public, **CO**=Confidential, only for members of the consortium (including the Commission Services), **CI**=Classified, as referred to in Commission Decision 2001/844/EC

Modifications Index	
Date	Version
26/ 05/2021	1.0 First version
07/06/2021	1.1 Quality Review
08/06/2021	2.0 Second version

This work is a part of the HYPERION project. HYPERION has received funding from the European Union's Horizon 2020 research and innovation programme under grant agreement no 821054.

ACRONYMS AND ABBREVIATIONS

CH	Cultural Heritage
HSI	Hyperspectral Images
GGS	Generic Ground Station
SAR	Synthetic Aperture Radar
UAS	Unmanned Aircraft Systems
RS-MMS	Remote Sensing-based Multiscale Monitoring System
HRAP	Holistic Resilience Assessment Platform
GCS	Ground Control Station
EMS	Emergency Management Service

Table of Contents

List of Figures

Executive Summary

The deliverable 6.4 focuses on the description of the novel methodologies for damage detection and assessment along the CH assets and the surrounding disaster affected area. The developed methodologies were evaluated on areas where natural disasters have occurred. The methodologies are applied according to a flowchart that provides the step-by-step approach for damage assessment in the broader area and the CH asset as well. Three flowcharts have been defined for three different disaster scenarios: flood, landslide and earthquake (chapter 2).

In chapter 3, the developed methodologies are described. The flood detection methodology is based on the detection of changes due to flood events exploiting the backscattering change between the pre-flood images and the flood image. The method consists of four main steps: a) data procurement b) pre-processing c) time series analysis and d) classification. The landslide detection methodology is based on ESA SNAP polarimetric functionalities for the delineation of a landslide. Entropy (H), Alpha (a) and Anisotropy (A) decompositions are calculated. An RGB composite based on the multitemporal ratio (before and after the event) is calculated. The delineation of the landslide is based on visual interpretation of the RGB composite.
The adopted technique for earthquake induced deformation is based on ESA SNAP functionalities for the detection of millimeter co-seismic surface displacements. Upon estimating the co-seismic ground deformation from ascending and descending geometries, a clear signal is identified and ground deformation is locally estimated.

Finally in chapter 4, the sensor strategies for damage assessment along the CH assets after disasters are discussed. Damage assessment includes the estimation of structural deformation as well as the detection of acute material deterioration. The consequences of limited sensor payload of currently available drones suitable for mobile deployment, and ways to balance information needs against abilities of different drone types and regulatory limitations are discussed in this chapter.

The deliverable is intended for public use, and it will particularly be helpful for the partners involved in the design of the HYPERION platform.

1. Introduction

1.1 Background

The deliverable D6.4 “Novel methodologies for damage detection and assessment along the CH assets and the surrounding disaster affected area” focuses on the post disaster monitoring and assessment of the CH assets and the surrounding area. The baselines for post disaster monitoring were set in D6.1 document as a part of the remote sensing-based multiscale monitoring system (RS-MMS) operational functions. In the same document, functions for the post disaster monitoring operation of the RS-MMS were defined according to three different scenarios, while data and methods for their development were reported. In document D6.4, the novel methodologies that have been developed within HYPERION project for the post disaster monitoring are being reported and their products are presented. For each disaster scenario, the processing flow is presented.

1.2 Scope and Objective

Objective of this document is the description of the novel methodologies that have been developed for three different disaster scenarios: flood event, earthquake, and landslide. For each scenario, an assessment of the situation on the broader area (including Tier 2 buildings and tier 3 infrastructures) is initially carried out, since CH assets (Tier 1) affected by a disaster do not exist in isolation and comprehensive event assessment requires the entire extent to be considered. To this end satellite data are processed through novel methodologies for damage assessment in the broad area and crosscheck with Copernicus EMS products (if available) is carried out for validation purposes. Satellite image processing is the first step in the processing flow and includes different methods for each disaster scenario.

The second step in the processing flow is related to damage assessment upon CH assets. Methods dealing with this issue are the same for all the scenarios and are already reported in D6.3. Close range mobile ground or airborne sensors will provide data as input for a detailed assessment of the CH asset state after the disaster. Comparison with a previous reference state (D6.3) leads to mapping not only severe but also slight damages of the assets’ structure and material. A dedicated sensor strategy including hyperspectral, photogrammetric and laser scanning sensors, has been adopted and evaluated through the development of advanced methods for 3D representation and material damage assessment (D6.2 and D6.3). This document also aims at providing an efficient sensor strategy for assessing damages after a disaster. The consequences of limited sensor payload of currently available drones suitable for mobile deployment, and ways to balance information needs against abilities of different drone types and regulatory limitations are discussed in this document, especially for fulfilling the needs described in the disaster scenarios.

2. The three disaster scenarios

2.1 Flood event

In case of a flood event, flood extent mapping and monitoring is required. The broader area should be inspected for the period of the event through the processing of satellite imagery. In case that Tier 1 buildings are found inside the flooded area, hyperspectral sensors on UAV should scan assets' facades and roofs. HSI processing will indicate acute effects of abnormally high concentrations of water and moisture increase on the roofs and facades of the monuments, which in relation to CH asset vulnerability will help stakeholders to make decisions.

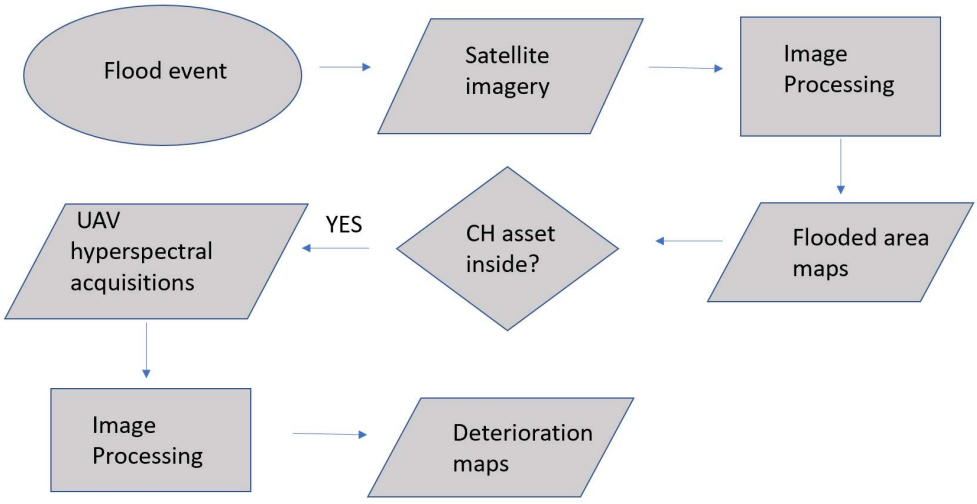

Figure 1: Flowchart for the flood event scenario

2.2 Landslide

Landslide will be mapped through satellite image processing. CH asset proximity to the landslide will serve as an indicator for operating ground and airborne sensors. The latter will provide data for assessing effects of landslides on the assets. 3D representations of the monuments will be created by acquiring aerial and terrestrial digital images in order to produce the point cloud of the CH asset and if needed the 3D surface. Comparison with reference data provided by the routine monitoring will produce 4D maps of the monument, in order to identify affected parts and estimate structural deformations.

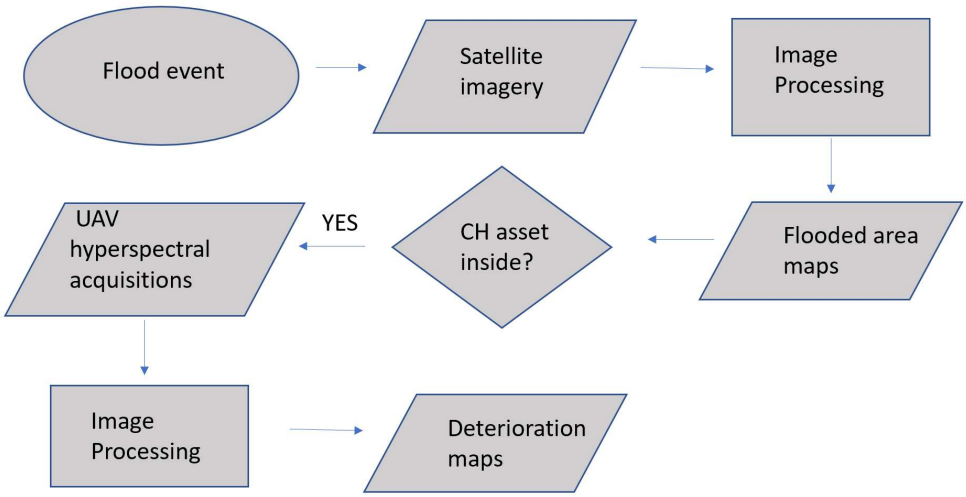

Figure 2: Flowchart for the landslide scenario

2.3 Earthquake-induced ground deformation

Land deformation caused by earthquake will be estimated using SAR satellite images. Mobile ground and airborne sensors (cameras mounted on drones) will be used in case that the earthquake epicentre is close to the CH assets. 4D representations will lead to structural deformation estimations and damage mapping, and will indicate maintenance interventions.

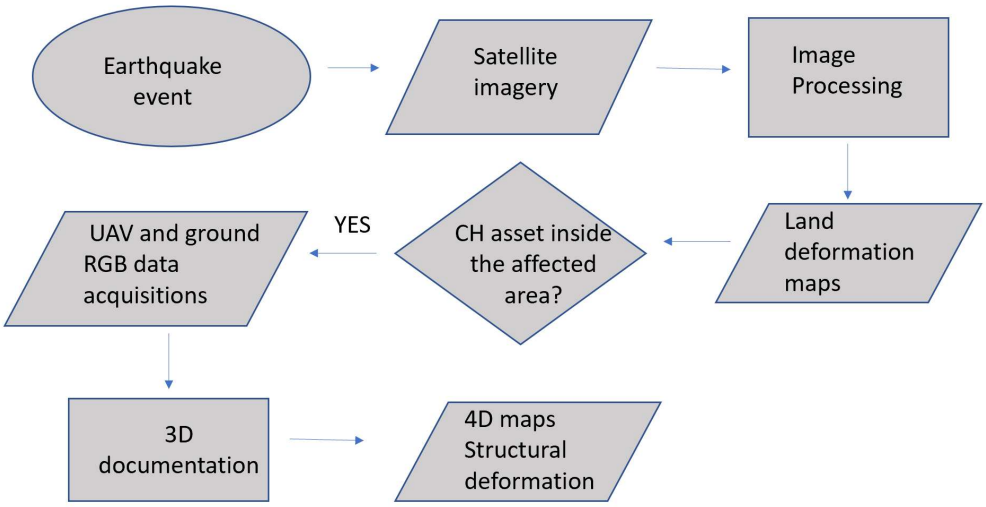

Figure 3: Flowchart for the earthquake scenario

3. Novel methods for damage assessment in the broader area

3.1 Flood mapping

Two different methodologies were developed addressing the different environmental complexities of urban and natural terrain respectively. We present one methodology over urban region (Venice, Italy) and another methodology over natural terrain (Kragero, close to Tønsberg, Norway)

3.1.1 Venice

Since 12 November, the Veneto region has been affected by a deep cyclonic circulation resulting in an intense phase of severe weather over Italian peninsula. The severe weather conditions caused a high tide in Venice, reaching the maximum value of 187 cm at 10:50 p.m. on the 12th of November, 2019.

The methodology was based on the change of the intensity information before and after the flood event. In particular, two pre-flood images (22/10/2019 & 28/10/2019) and one post-flood image (15/11/2019) were selected. All the images are from the same descending orbit track (relative orbit 95) of Sentinel-1 (C band, 5.546 cm wavelength). The extracted flooded area is a result of change detection approach between pre- and post- flood information. The change detection algorithm consists of two main steps. In the first step, a probability distribution of the pre-flood intensity is modelled for each small patch (5x5 pixels). In the second step, for each patch, the post-flood information is checked if it belongs to the modelled step-1 distribution for a confidence interval of 95%. In the following map, possible flooded areas are denoted with blue color.

Figure 4: Flood map results over Venice pilot area

We highlight that the medium resolution SAR data (Sentinel-1, 10m) over urban areas are noisy due to the complex urban structure. Consequently, we provide the extracted changes as a proxy to the flood affected areas.

3.1.2 Kragero

In this section we present the methodology and produced results regarding a flood event over a natural terrain region (lake Bjorvann, Kragero, Norway). Heavy rains in the Kragero region have raised an orange level flood alert in the area. Many landslides events are expected, some with considerable consequences, as well as extensive flooding, erosional damage and flood damage in prone areas.

The methodology that was developed consists of the following steps:

1. Data procurement

Starting with a predefined area of interest and flood event time we analyzed all available Sentinel-1 acquisitions. We select the optimal orbit track for analysis based on the time difference between acquisition time and the end time of the flood event. The acquisition right after the end time of the flood event is treated as the “flood” image. Next, we form a baseline (pre-flood) dataset by using the acquisition of the last three months. Based on historical precipitation data (ERA-5), we discard the acquisitions that are related to high cumulative (5 days before the acquisition time) precipitation.

2. Pre-processing

The pre-processing steps (based on ESA Sentinels Application Platform SNAP functionalities) consists of the following steps:

- Apply orbit correction. In particular, restituted orbit files were applied to the images, resulting in geometric accuracies within 10 cm (Prats-Iraola et al., 2015).
- Border Noise Removal which masks artificially low backscatter pixel found at the edge of the image swath (Ali et al., 2018).
- Radiometric calibration was performed to produce unitless backscatter intensity (Sabel et al., 2012)
- Subsetting at given AOI spatial extends.
- Co-registration between all images in order to create a stack that will be used for time series analysis.
- Terrain geocoding using the 1-arcsec digital elevation model (DEM) from the Shuttle Radar TopographyMission (SRTM) .
- Conversion of the unitless backscatter coefficient is converted to dB using a logarithmic transformation (Filipponi, 2019).

3. SAR statistical temporal analysis

After the preprocessing, a statistical temporal analysis between baseline (pre-flood) stack and "flood" image is performed. The t-score was selected due to the small sample size and is calculated for each pixel following the formula:

$$t_{score} = (\sigma_{flood} - mean\sigma_{baseline})\sqrt{n}/std\sigma_{baseline}$$

Where,

σ_{flood} the backscatter coefficient of the "flood" image

$mean\sigma_{baseline}$ and $std\sigma_{baseline}$ the average value and the standard deviation of the backscatter coefficient of the baseline (pre-flood) stack, respectively

n the number of the acquisitions in the baseline stack

4. Classification

A novel classification scheme was developed in order to detect the flood affected areas. The main input is the t-score image between baseline (pre-flood) stach and "flood" image. The classification scheme consists of six main steps.

- Calculation of bimodality mask. Create a mask with regions that consists of two or more populations (Freeman et al., 2013). In our case, our populations are floodwater and non-floodwater.
- Gaussian mixture modelling of the two populations based on least squares.
- Global thresholding based on Kittler-Illingworth Thresholding algorithm (Kittler et al., 1985).
- Spatial adaptive local thresholding in order to compress overdetection issues and reduce commission errors.
- Region growing in order to compress underdetection issues and reduce omission errors.
- Refinement which consists of a) masking out high slope regions from available DEM and b) morphological filtering based on a predefined minimum mapping unit.

For the case study we used 6 pre-flood images (04/09/2017, 16/09/2017, 22/09/2017, 28/09/2017, 10/10/2017, 16/10/2017, 22/10/2017) and 1 "flood" image (22/10/2017). All the images are from the Sentinel-1 ascending track (relative orbit 44) with C band (5.546 cm wavelength). The results of our case study in Kragero are presented in the following Figure.

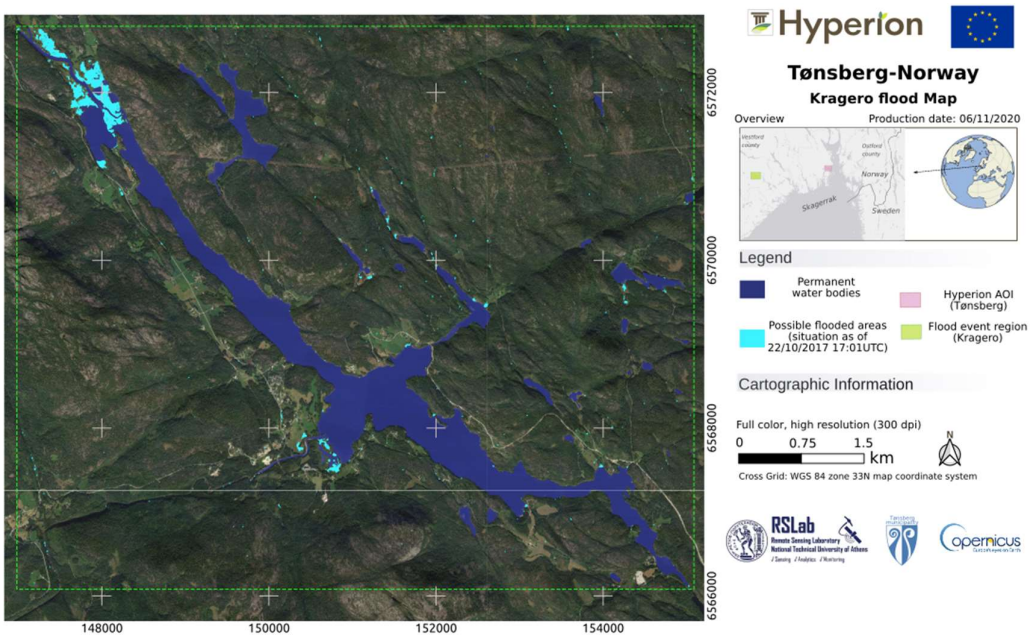

Figure 5: Flood map results over Kragero (close to Tønsberg pilot area)

3.2 Landslide mapping

Due to the absence of landslide events close to pilot areas, the Maoxian landslide in Mao county, Sichuan Province, China was selected. The landslide occurred in the early morning of 24 June 2017 and killed more than 100 people in the village of Xinmo.

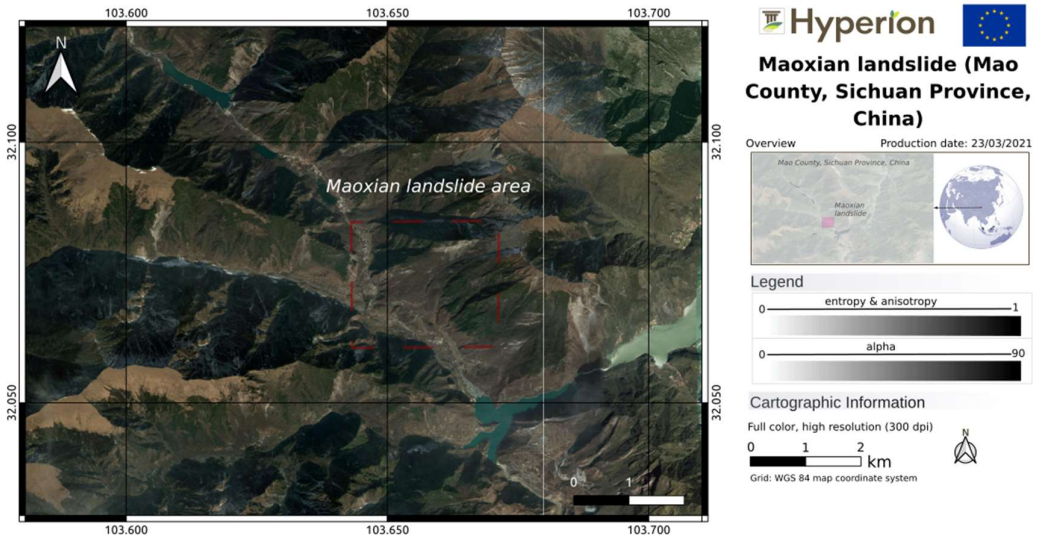

Figure 6: Location of Maoxian landslide area

A novel methodology based on polarimetric SAR principles was developed. Polarimetric SAR methodologies are commonly used in order to estimate forest and crop parameters (Nasirzadehdizaji et al., 2019; Wang et al., 2020). We extended these methodologies in order to map the affected area of a landslide using a two-step

approach. In the first step an Entropy (H)- Alpha (a)-Anisotropy (A) decomposition is calculated for an SAR image before and after the landslide event.

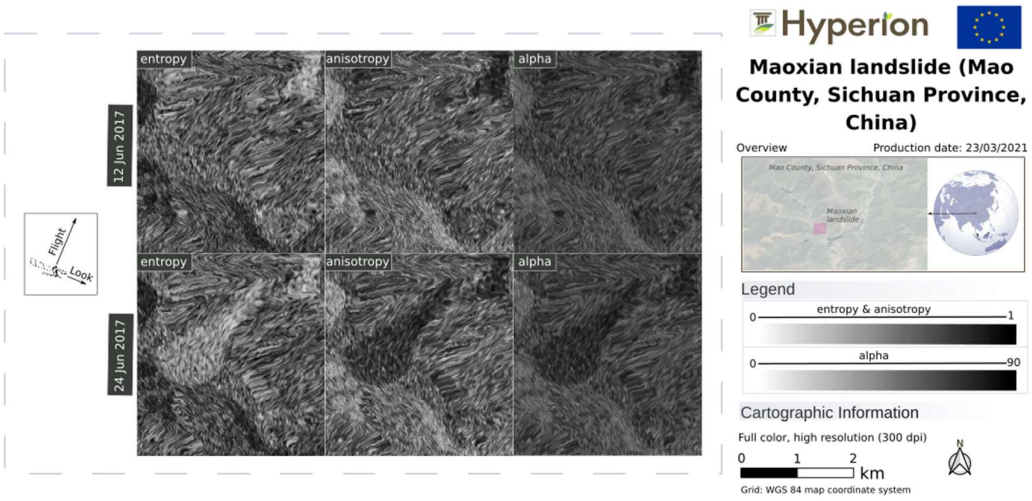

Figure 7: Polarimetric results (step-1) of the proposed methodology

In the second and final step, an RGB composite based on the multitemporal ratio (before and after the event) was calculated. The described processing scheme was implemented using ESA SNAP functionalities. The processing scheme supports the processing of Sentinel-1 Terrain Observation with Progressive Scans (TOPS) datasets and uses the SRTM 1 Arc-Second (30m resolution) elevation data. The delineation result of the proposed method was validated using an optical Sentinel-2 image.

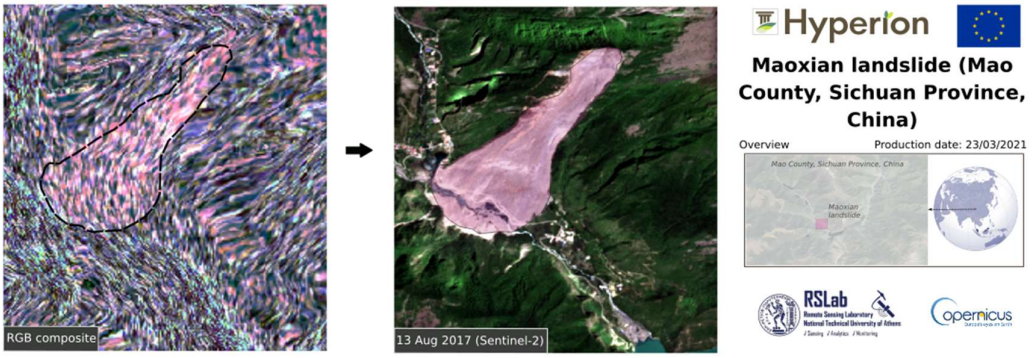

Figure 8: Delineation results (step-2) of the proposed methodology and validation with Optical data

In the above figure, we demonstrate that the delineation of the landslide affected area from the proposed methodology strongly agrees with the hand-digitized result from optical (Sentinel-2) data.

3.3 Earthquake-induced land deformation

Due to the absence of strong earthquake events close to pilot areas, the Kos-Greece M6.6 earthquake at 20/07/2017 in the vicinity of Rhodes pilot area was selected. The methodology was based on InSAR principles. In particular, a multi-orbit processing scheme based on ESA SNAP functionalities was implemented. The processing scheme supports the processing of Sentinel-1 Terrain Observation with Progressive Scans (TOPS) datasets and uses the SRTM 1 Arc-Second (30m resolution) elevation data. Ground deformation results are referring to the Line of Sight (LOS) sensor to target direction. The following results demonstrate that we are able to detect coseismic ground surface displacements at a high (up to millimeter) accuracy.

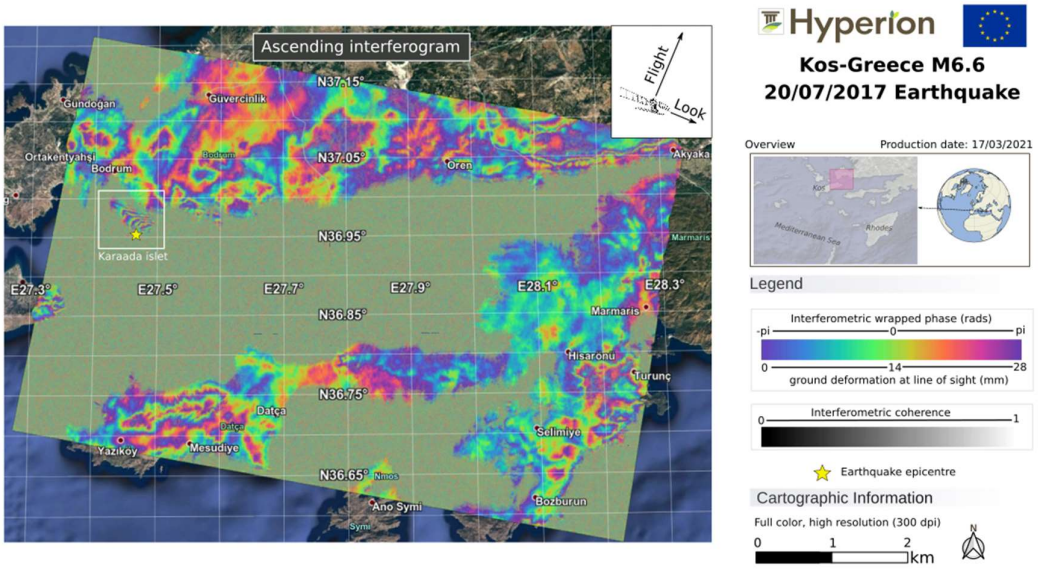

Figure 9: Ground deformation results from ascending geometry

In the above figure, the ground deformation results from Sentinel-1 ascending track 131 data are presented. In particular, the wrapped interferometric phase information between 12/7/2017 and 24/7/2017 is visualized. One fringe of Sentinel-1 C-band interferogram corresponds to half wavelength, i.e. 28 mm. A clear signal mostly located in the Karaada islet (white box) was identified. A signal is localised in the Karaada islet and corresponds to a ground deformation of eight fringes (~0.224 m).

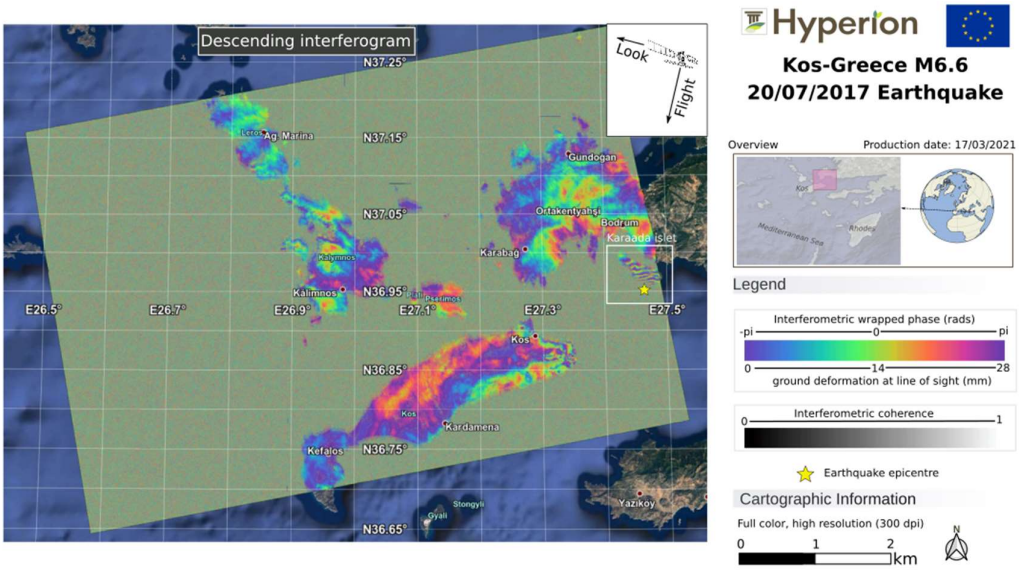

Figure 10: Ground deformation results from descending geometry

In the above figure, the ground deformation results from Sentinel-1 descending track 31 data are presented. In particular, the wrapped interferometric phase information between 18/7/2017 and 24/7/2017 is visualized. A clear signal mostly located in the Karaada islet (white box) was identified. A signal is localised in the Karaada islet and corresponds to a ground deformation of seven fringes (~0.196 m).

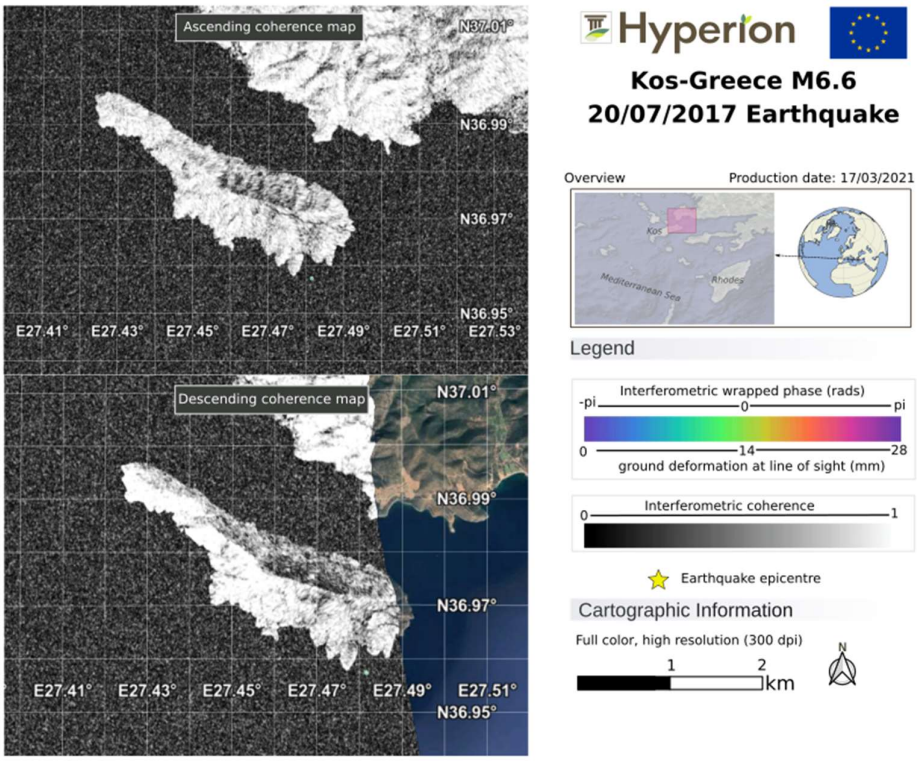

Figure 11: Quality (coherence) maps of ascending and descending ground deformation

In the above figure, the quality maps of the ground deformation results for each geometry are presented. The interferometric coherence was used as a quality index of the extracted ground deformation. Values close to 1 (bright tones) correspond to high quality, where values close to 0 (dark tones) correspond to poor quality. The bright tones of the Karaada islet means that we have a high quality of the ground deformation results for both geometries.

4. Sensor strategies for damage assessment

4.1 Sensor strategies for structural deformation assessment

The estimation of the structural deformation is crucial for damage assessment not only for routine monitoring but mostly after a disastrous event. The equipment that will be used for the 3D documentation of the damaged CH asset and the methodology that will be followed for both the data acquisition and the data processing need to give fast and accurate results.

The best and recommended practice is to use transportable, light and flexible equipment that can be used even when the CH asset cannot be physically accessed after an event. The main components of the GCS will be used for this case utilizing multi-rotor and/or fixed aerial vehicles combined with multispectral sensors. Authorized drone pilots can get easily and fast the necessary permission to perform flights at the damaged areas and acquire the necessary digital images. In order to properly document the CH asset both manual and pre-programmed flights will be executed, using the flight plans of the initial 3D documentation and focusing on the damaged parts of the buildings. The mapping parameters like the image overlap, camera angle and flight altitude will be properly adjusted according to the needs and complexity, while the information of the initial flight plans will be used as guidelines for this process.

The acquired data will be instantly transferred and stored to the GCS laptop via the wireless connection and the remote controllers of the UAS. This way the data processing can be almost in real time by importing the stored digital images into the Image Based Modelling (IBM) software, e.g., Agisoft Metashape, of the GGS. These images will also be available to certain users of the HRAP platform that need to get a better insight of the damage and the CH assets. The data processing procedure will focus only on the development of the dense point cloud of the CH asset in order to get accurate results in a very short time. The captured images will be aligned and the sparse point cloud will be edited in the software using the available filters in order to reduce the inevitable noise and improve the results of this automatic process. After the successful alignment of the digital images, the initial 3D point cloud or mesh will be used as reference to acquire coordinates for specific points that present no damage or deformation close to the CH asset. That way the sparse point cloud will be georeferenced to the same coordinate system as the reference 3D point cloud. The

next step of the process will be to generate the dense 3D point cloud and once again apply the available filters of the software in order to edit it and remove the noise.

The proposed methodology will give accurate and fast results leading to the comparison of the 3D point cloud with the reference one after an event. The two point clouds will be imported into the CloudCompare software (open-source) and a cloud to cloud comparison will be performed to estimate the structural deformation of the CH asset. To further support the results it is recommended to compute statistical analysis by fitting a distribution on the distances using the Scalar fields tool and the Computation of statistical parameters. The mean distance, the standard deviation, the minimum and maximum values will be available for each case, while the results and the distances will be exported and a report will be generated. Finally, a more advanced tool will be used for the comparison, the qM3C2 plugin of CloudCompare. This plugin is the unique way to compute signed and robust distances between two point clouds and it also provides the precision maps.

In this section it is important to mention some restrictions that may arise in this process. Due to weather conditions or official flight restrictions, it is possible that the UAS may not be able to execute a flight right after an event. The authorized pilots are able to overcome these obstacles by applying to the appropriate authorities and getting and official permission to perform the necessary flights. Moreover, various UAS aircrafts can be used for the data acquisition process that present a better wind resistance, otherwise the flights could be performed with the suitable weather. Another challenge for the UAS could be any obstacles close to the CH assets or high trees that may cover the buildings. The aircraft will not be able to fly close to them leading to lack of information. For these parts of the CH assets images can be taken from the ground using a handheld camera and combining these data with the aerial ones.

4.2 Sensor strategies for acute material deterioration effects after an event

As exhibited in Kolokoussis et al 2021 the integration of the 3D and hyperspectral (HS) data lead to interesting conclusions on the vulnerability of the building materials as well as the role of the biodeterioration factors in material loss. After a disastrous event the integration of 3D with HS data may reveal the most vulnerable parts of a CH building which have to be given the highest priority for supporting or repairing actions. Moreover, certain events like flood, frost or other extreme bioclimatic conditions could cause changes that are not observable by visual inspection while can be detected and mapped with the use of HS imagery. A fast and low cost HS mapping of the CH asset would be desirable in such circumstances.

Handheld HS imaging devices could be used for fast inspection of the CH asset, although the best and recommended practice is to use transportable, light and flexible HS equipment that will follow the same image acquisition pattern with the sensors used for the 3D documentation. Thus, it is better that the relevant HS imaging devices

will also be appropriate to be installed on a UAV, which is even more crucial when the CH asset cannot be physically accessed after an event. Furthermore, since imaging of the facades of the buildings are of more important than vertical acquisitions these HS imaging devices is better to adopt snapshot imaging rather than pushbroom technology. The HS cameras that have been used in the Rhodes experiments comply with this requirement, but their spectral resolution is faint and the very demanding pre-processing and processing required make them inadequate for near real time or fast response applications. Not only higher spectral resolution imaging devices are required for such applications but furthermore it is better that these imagers will cover a wider spectral range from visual to middle infrared, since many relevant publications indicate that the middle infrared part of the spectrum is very useful for the detection of various deterioration factors.

A pre-built spectral library, concerning all the deterioration factors and the stone materials, and compatible with the HS imaging devices used, should be available in order to speed up the HS analysis (i.e. spectral unmixing) and mapping process, providing results in near real time, which can then be draped on the 3D model in order to draw safer conclusions about the condition of the affected CH asset. If the HS imaging devices adopt the snapshot technology, software solutions like Agisoft metashape, Pix4D, etc can also be used in order to be used for producing a rougher but HS enriched 3D model.

As far as it concerns the data transfer as well as the flight parameterization and limitations they are the same with those denoted for the 3D documentation in the previous section.

5. Conclusions

Three flowcharts have been defined for three different disaster scenarios: flood, landslide and earthquake. For these scenarios, three novel methodologies have been developed and applied on satellite data, respectively, for assessing the areas affected by the disasters. Evaluation of the methodologies showed that they can successfully assess the affected areas. The novel methodologies developed for the damage assessment of the CH assets and specifically for the structural deformation assessment focused on the methodology for both the data acquisition and the data processing. The proposed methods for the 3D modelling and comparison with the reference data will give fast and accurate results which is the most crucial fact after an event.

6. References

Ali, I., Cao, S., Naeimi, V., Paulik, C., & Wagner, W. (2018). Methods to remove the border noise from Sentinel-1 synthetic aperture radar data: implications and importance for time-series analysis. IEEE Journal of Selected Topics in Applied Earth Observations and Remote Sensing, 11(3), 777-786.

Filipponi, F. (2019). Sentinel-1 GRD preprocessing workflow. In Multidisciplinary Digital Publishing Institute Proceedings (Vol. 18, No. 1, p. 11).

Freeman, J. B., & Dale, R. (2013). Assessing bimodality to detect the presence of a dual cognitive process. Behavior research methods, 45(1), 83-97.
Kittler, J., Illingworth, J., & Föglein, J. (1985). Threshold selection based on a simple image statistic. Computer vision, graphics, and image processing, 30(2), 125-147.

Kolokoussis P., Skamantzari M., Tapinaki S., Karathanassi V., Georgopoulos A. (2021). 3D and Hyperspectral data integration for assessing material degradation in medieval heritage buildings. Submitted and accepted for publication in the proceedings of the XXIV ISPRS Congress.

Nasirzadehdizaji, R., Balik Sanli, F., Abdikan, S., Cakir, Z., Sekertekin, A., & Ustuner, M. (2019). Sensitivity analysis of multi-temporal Sentinel-1 SAR parameters to crop height and canopy coverage. *Applied Sciences*, *9*(4), 655.

Prats-Iraola, P., Nannini, M., Scheiber, R., De Zan, F., Wollstadt, S., Minati, F., ... & Desnos, Y. L. (2015, July). Sentinel-1 assessment of the interferometric wide-swath mode. In 2015 IEEE international geoscience and remote sensing symposium (IGARSS) (pp. 5247-5251). IEEE.

Sabel, D., Bartalis, Z., Wagner, W., Doubkova, M., & Klein, J. P. (2012). Development of a Global Backscatter Model in support to the Sentinel-1 mission design. Remote Sensing of Environment, 120, 102-112.

Wang, J., Li, K., Shao, Y., & Wang, Z. (2020, October). Monitoring of rice lodging using Sentinel-1 data. In *Journal of Physics: Conference Series* (Vol. 1651, No. 1, p. 012080). IOP Publishing.